Low-Noise Switched Reluctance Drive

Debiprasad Panda, V. Ramanrayanan
Department of Electrical engineering
Indian Institute of Science
Bangalore 560012
India
email:dpanda,vram@ee.iisc.ernet.in

Abstract:

Switched Reluctance (SR) Motor Drive is of great topical interest. It has the potential to emerge as a viable option for variable speed applications. Though simple in construction, the motor is quite rugged, and has many attractive features like high torque-to-inertia ratio, fault tolerance, and high efficiency. A number of converter topologies are prescribed for driving the motor. However, its applicability is limited because it emits high acoustic noise in operation. This paper deals with the issues regarding sources of acoustic noise, and means of reducing the same, and finally proposes a low-noise control algorithm based on voltage control. It achieves noise abatement by the use of a TMS320c50 based DSP platform. The controller was tested on a 5 hp 8/6 OULTON motor. Results of tests, measurement of noise level at different speeds, and performance comparison with an existing system are presented.

1. Introduction

SR motor is doubly salient, its stator alone is excited, and the rotor has no windings. The torque is produced by the tendency of the rotor to orient along the minimum reluctance position on excitation, and does not depend on the direction of the current through the winding. Thus an unipolar converter is sufficient to drive the motor. The efficiency of the motor is high. It has many interesting features to become a drive of future. The working principle of the motor is well documented in literature [1-3]. One of the major limitation of this motor is that it emits high acoustic noise.

2.0 Acoustic noise

There are stringent specifications governing the acoustic noise levels of industrial and household applications. The conventional SR motor drive, especially at low speeds, has a higher noise level than conventional motors. The possible noise sources in SR motor are discussed below.

i) Radial Force

There is a strong radial magnetic attraction between the stator and the rotor of the SR motor because of the doubly salient structure. The stator vibration is found to be proportional to the rate of demagnetisation. During commutation, when the phase winding is demagnetised, the stator vibrates, and this vibration produces high acoustic noise. The radial force F_r [4] can be expressed by

$$F_r(\theta, l_g, t) = -\frac{1}{2} i(t)^2 \frac{L(\theta(t), i(t), l_g)}{l_g} \quad (1)$$

where θ is the rotor position, l_g is the minimum airgap between the stator and the rotor at the aligned position, L is the self-inductance of the winding, and i is the winding current. Due to the radial force the rotor may take different vibrating modes. Most common of them is the oval shape. The stator is compressed along the axis of the excited stator poles and expanded along the quadrature axis. The typical shape is shown in Fig. 1.

ii) Torque ripple

Under conventional control algorithms, the SR motor exhibits considerable torque ripple which is a potential source of noise.

iii) Winding vibration

Winding vibration produced by the interaction of current in the stator windings with leakage flux ($I \times B$ - Lorentz Force) is also a source of noise.

iv) Compressions under magnetic effect (Permeance variation)

Magnetostrictive forces are present in all compressible magnetic materials under the influence of a magnetic field. These forces are generated by the tendency of the magnetic circuit to adopt a configuration of minimum energy. These forces compress the material and thus increase its effective permeability. The vibration in all parts of the magnetic material caused by this force also produces noise.

v) Mechanical imperfections:

Faulty bearings and other mechanical defects also lead to noisy vibration.

2.1 Means of acoustic noise reduction: voltage control

Several researchers [4-8] have carried out extensive experiments into the nature, intensity, and means of control of different sources of noise in SR motors. Their experiments reveal that the vibration of the stator induced by radial magnetic forces is the dominant source. The noise peaks when the harmonics of the radial force and resonance frequencies of the stator

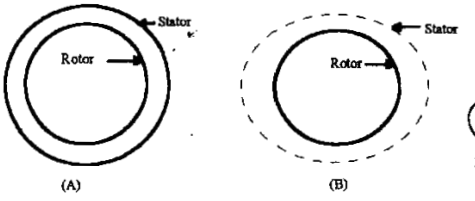

Fig. 1 Ovalization of the stator due to the radial force, (A) Normal condiotion (without any excitation, (B) Under excited condition.

coincide. As explained in point *(i)*, it is the rate of withdrawal of radial force that decides the level of noise. So, a gradual release of the force should reduce the noise. From Eq. 1, it is clear that radial force F_r is a function of rotor position as well as i^2. As the position of the rotor gets closer to the aligned region during commutation, the noise increases. Similarly, if the current in the winding is extinguished instantaneously by applying a higher negative voltage across the phase, the noise will be very high. The implication is that noise can be brought down considerably by controlling the current gradient. The current gradient can be made gradual by nonapplication of full voltage across a winding and by making the DC bus voltage a function of speed. Thus the voltage control method is a desirable and feasible option for noise abatement in an SR motor.

The SR motor can be subjected to either current control or voltage control [2]. In the current control mode, the DC bus voltage is kept constant to the rated value and the currents of individual phases are controlled by hysteresis control or by constant frequency chopping in the low speed region and conduction angle control in the high speed region [2, 3]. Though the control of the SR motor is easier and faster in the current control mode, at low speeds, full voltage comes to be applied across the winding, resulting in large current gradients that increase the acoustic noise.

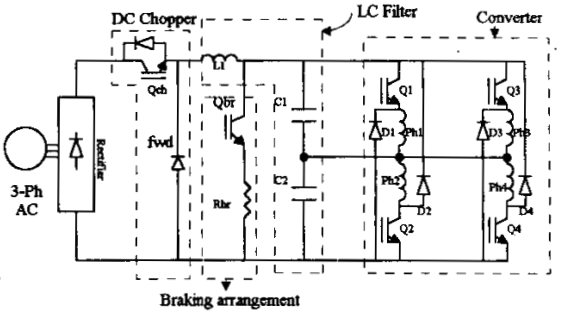

Fig.2 Converter for SRM

In the method proposed in this paper, a chopper circuit is incorporated between the rectifier and the power converter of the SR motor (c.f. Fig. 1). Thus the motor is supplied with variable voltage. This variable voltage is made a function of speed so that it is capable of maintaining sufficient current in the presence of the back emf. In such a method, the current gradient in the windings is substantially reduced. Thus voltage control reduces the noise to a level considerably lower than in current control. Further, the machine is controlled in single-pulse, which makes it is eminently suited to sensorless operation [9]. The proposed control scheme is thus capable of giving higher-accuracy information of position [9], and reducing the noise level.

3.0 Realisation of the controller

A TMS320c5x-based DSP-board is used for the implementation of the algorithm proposed here. The DSP gathers the position informations from four discrete optical sensors, mounted on the shaft of the motor. These signals are processed by the DSP, and the DSP provides five switching signals, one for each of the four phases of the motor, and one switching signal for the DC chopper switch control through a digital I/O port. The total control including speed calculation, choosing appropriate T-on and T-off angles, control of chopper duty cycle etc. is effected by the DSP.

The total control block diagram is shown in Fig. 3. The commanded speed Wref is compared with the

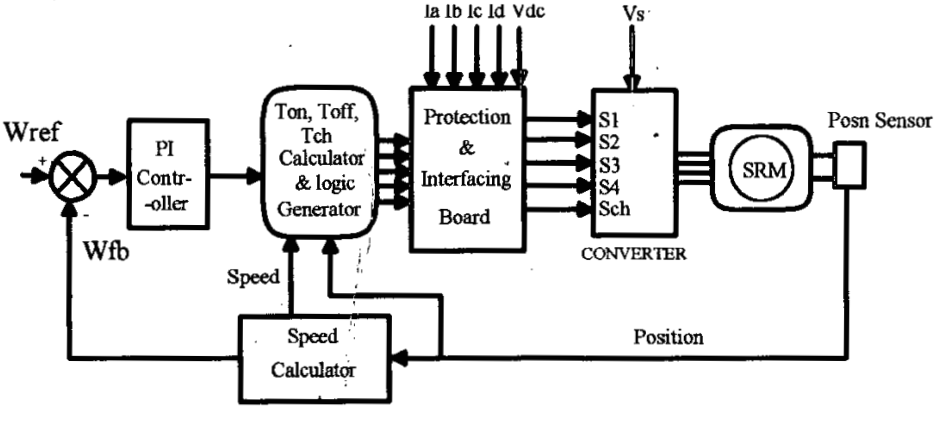

Fig. 3. Control Block Diagram of SRM

5. System Synthesis

The current open loop transfer function is simplified as a first order delay plant after compensation. The system block diagram after compensation is shown in Fig.9.

The model in Fig.9 is a low frequency model. Although it can not provide high frequency

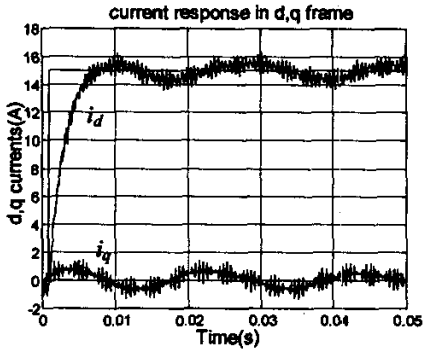

Fig 8 (a)

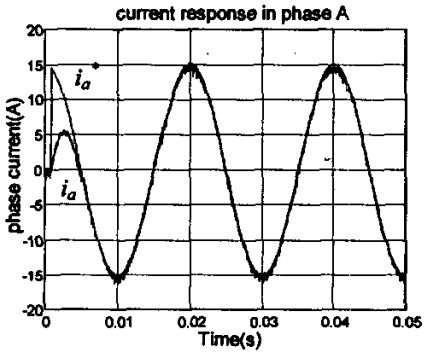

Fig.8 (b)

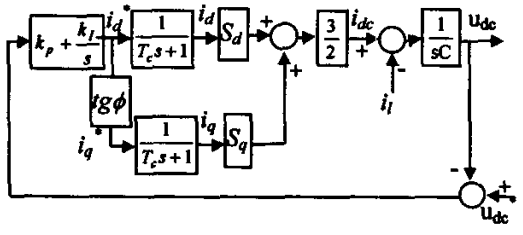

Fig.9 block diagram of dynamic decoupled rectifier

harmonic information as expression(5) and (6), it is precision enough to study on the system dynamic characteristics, stability and takes less computing time in simulation. Fig.9 is a gain variable system because S_d and S_q depend on load condition. It is difficult to synthesize a system shown in Fig.9. A viable method is to linearize the system at different steady point.

In most application, unity power factor is need. In other words, tgϕ is equal to zero . The q axis current branch can be negligible and the transfer function can be somewhat simplified. Following analysis based on a unity power factor rectifier.

In phase minimum system, open loop gain increasing leads to stability decrease. A robust controller must ensure the stability of system even in the worst condition. It can be seen from expression (9),(10) and Fig.4 that S_d takes its maximum value at unload condition if tgϕ is equal to zero. where:

$$\max[S_d] = \frac{u_{sd}}{u_{dc}} \qquad (24)$$

Fig.9 is a phase minimum system, so the system will be stable at any load condition if the controller can make the system stable at unload condition. The open loop transfer function at unload condition is:

$$\frac{\frac{3}{2}\cdot\frac{1}{C}\cdot\frac{u_{sd}}{u_{dc}}\cdot k_I\left(\frac{k_p}{k_I}s+1\right)}{s^2\left(T_c s+1\right)} \qquad (25)$$

Increasing capacitor and dc voltage reduce the open loop gain and increase the stability. On other hand, the voltage response speed will be decreased.

Utility voltage rises lead to the rise of open loop gain. So the voltage response speed will increase too, while the penalty is the stability decreased.

If S_d is taken value at unload condition, The voltage controller design is a typical synthesis problem of a second order plant. There are two integral items and a first order delay item in the denominator. The phase lag of denominator had extended out of -180°. In order to make system stable and provide enough phase margin, it seems that k_p must be much larger than k_I. But simulation shows that k_I can be set much larger than k_p. The reason is that the controller output exist saturation feature. Saturation is a nonlinear feature. When controller worked in saturation situation, integral operation stopped, that means

actual speed Wft; the difference between these two is the speed error. This error is fed to a PI speed controller. The output of the PI controller determines the T-on angle. The T-on angle is advanced towards the unaligned region if the error is positive, and towards the aligned region if it is negative. If the error is zero, there is no change in the switching angle. The T-off angle is a function of speed. The lower the speed, the closer it is to the aligned position. The variation of the Turn-off angle is kept within a narrow band (18.75°-22.5°), whereas the T-on angle ranges widely, i.e. from -7.5° to +12.5° . The DC bus voltage is a function of speed. Depending on the speed, the DC bus voltage is varied between 5% and 95% of the supply voltage. The full voltage across the DC bus is 600V. The duty ratio of the chopper circuit is decided by the speed of the motor. The machine is loaded through a DC machine coupled to its shaft. The rotor position information can be obtained from a position sensor or indirectly can be estimated using the flux-linkage characteristics of the motor [9].

4.0 Results

First the performance of the drive is studied through simulation. For that a commercial software package SIMULINK is used. The measured flux-linkage characteristics of the motor is used for modelling the motor. Through simulation the T-on and T-off angles for different load and speed are obtained. The voltage required for different speed is also found from the simulation. Then using the above control parameters the proposed method is implemented on a DSP, and the drive is tested throughout the speed and load range. The simulated and experimentally obtained voltage and current waveforms at different speeds and loads are shown in Fig. 4 & 5. The results obtained through simulation and experiment are quite close.

4.1 Acoustic noise measurement

The acoustic noise is measured with a *Bruel & Kjaer* 2235 Precision Sound Level Meter. The sound meter is kept 1 metre away from the motor axis in the radial direction. First the sound level is measured at different speeds (experiment A) of the DC motor. Then the SR motor is driven by a commercial drive controller (OULTON motor and controller manufactured by M/s Tasc Drive of UK) and the noise level is measured at different speeds (Experiment B). Finally the SR motor is driven by the proposed controller and the sound level measured at different speeds (Experiment C). The environmental noise during the experiment is noted separately (58 dB). The additional noise caused by the DC motor (Experiment A) is subtracted from the noises of Experiment B and Experiment C. The remainder figures can be taken as the noises due to the SR motor. The experiments are repeated for different loads

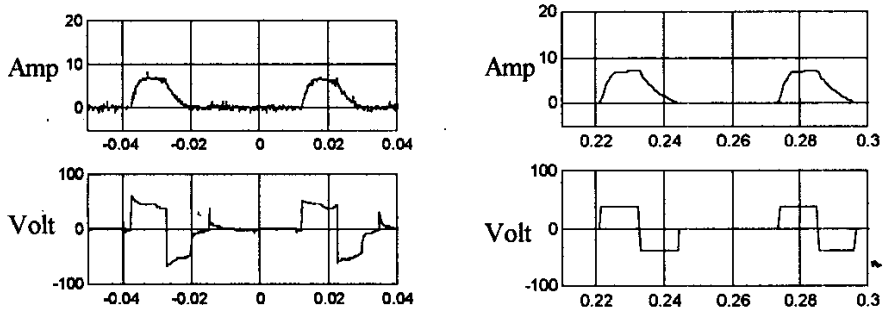

Fig. 4a Experimental (left) and Simulated (Right) Current (Top) & Voltage (Bottom) in volt Waveforms at 200 rpm at 5 Nm load

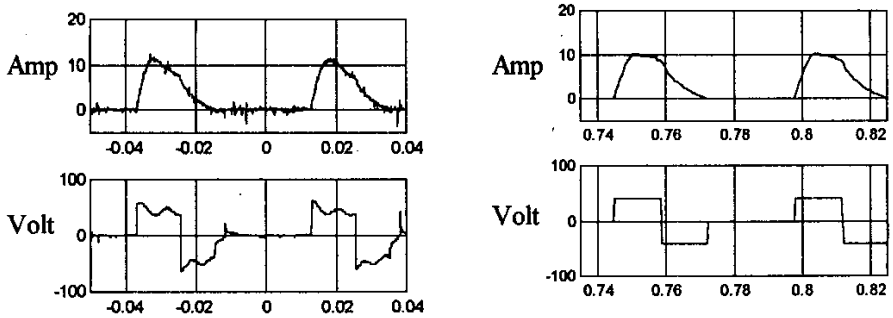

Fig. 4b Experimental (left) and Simulated (Right) Current (Top) & Voltage (Bottom) Waveforms at 200 rpm at 10 Nm load

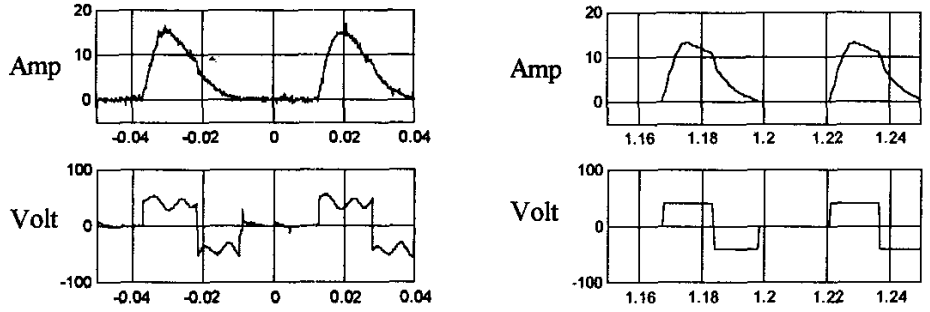

Fig. 4c Experimental (left) and Simulated (right) Current & Voltage Waveforms at 200 rpm and at 15Nm load

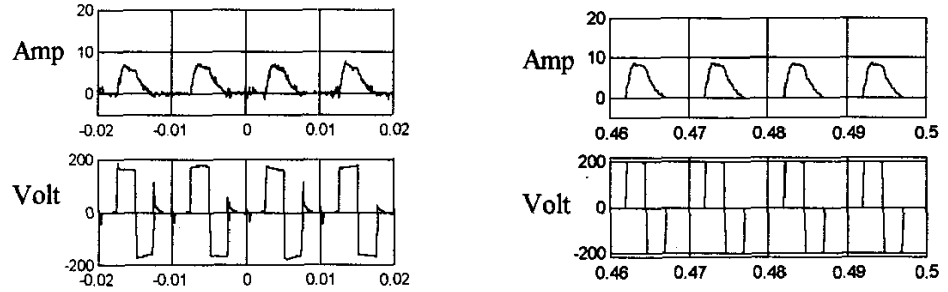

Fig. 5a Experimental (left) and Simulated (right) Current & Voltage Waveform at 1000 rpm and at 5 Nm load

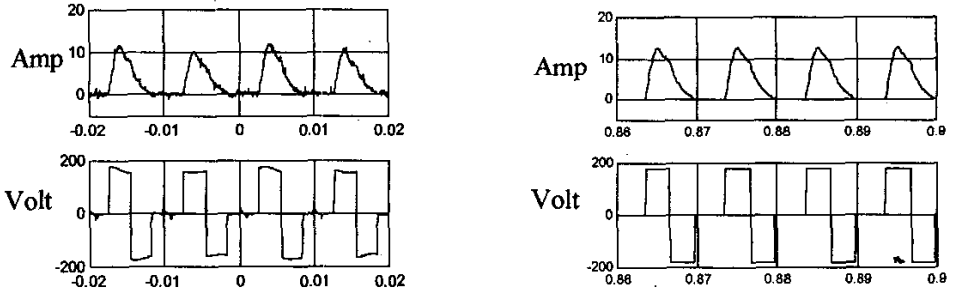

Fig. 5b Experimental (left) and Simulated (right) Current & Voltage Waveform at 1000 rpm and at 10 Nm load

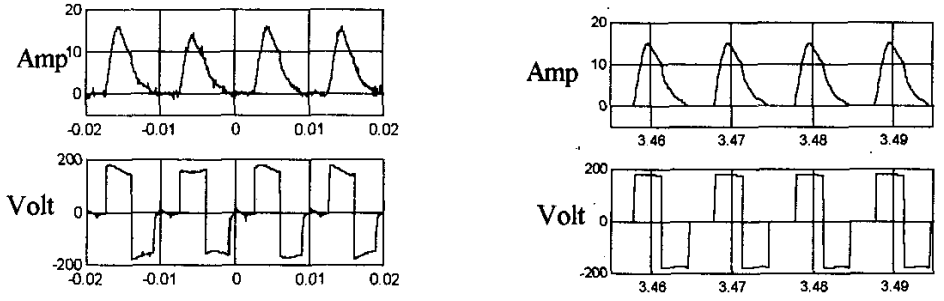

Fig. 5c Experimental (left) and Simulated (right)Current & Voltage Waveform at 1000 rpm and 15 Nm load

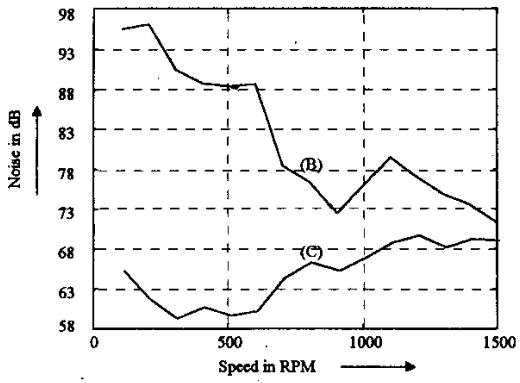

Fig 6. Noise level in dB for the OULTON drive (B) and the Proposed Drive (C)

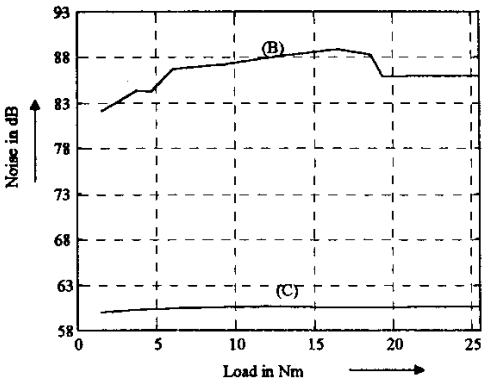

Fig. 7. Noise level in dB for the OULTON drive (B) and the proposed drive (C) at different loads for 500 rpm

(25%,50%,75% and 100% load). It is not the case always that the noise level at its highest under full-load condition of the motor. The highest noise levels reached by the conventional drive (B) and the proposed scheme (C), at different speeds (from 150 rpm to 1500 rpm) are shown in Fig. 6. The results clearly show that the proposed method is superior to the conventional control method at low and medium speeds. At high speeds (near the rated speed), however, the difference is not significant as the supply voltage and the conduction angle are the same. The small improvement in noise at rated speed (see Fig. 4) may be due to the difference between the schemes with respect to T-on and T-off angles [4]. It is also observed that in the OULTON drive, the noise at a particular speed varies with the load. The noise level variations of the OULTON drive at different loads and the same speed is shown in trace B of Fig. 7. A variation of 6 dB is observed. In the scheme proposed here, the noise level is almost constant at this speed under different loads (see trace C of Fig. 7). The OULTON motor and the TASC drive used here are fifteen years old in design. After that a lot of work has been done to reduce the noise level of the SR motor by redesigning the motor [8]. But the point to be noted here is that the control scheme proposed here has dramatically reduced the noise level of the same motor based on the old design.

4.2 Transient response:

The transient speed responses following the above method is plotted in Fig. 8. The response time obtained is of the order of seconds, which is obviously higher than fixed voltage current control mode [10]. However this method can be used where the dynamic performance criterion is not very stringent.

5.0 Conclusion

The discussion makes it clear that by adopting voltage control, single-pulse mode of control of SR motor is possible from very low speed to high speeds. This control method inherently leads to an appreciable reduction of noise at low speeds, where otherwise it is very high. The noise is measured ranging from 150 rpm to 1500 rpm in steps of 100 rpm for different load conditions and the noise level is found to be always within 70 dB (including the background noise of 58 dB), which is quite modest and acceptable. The single pulse operation also helps obtaining simpler position estimation algorithm. The present scheme can be utilised in household appliances like washing machines, mixers, grinders and vacuum cleaners.

6.0 References:

1. P.J.Lawrenson, J.M.Stephenson, P.T.Blenkinsop, J.Corda and N.N.Fulton, "Variable-speed switched reluctance motors", Proceedings IEE Vol 127, Pt.B, No. 4, pp- 253 to 265, July 1980.

2. Miller T.J.E.,"Switched Reluctance Motors and Their Control", Magna Physics Publishing And Clarendon Press Oxford 1993.

3. Bose B. K. , Miller T J E, Szczesny PM, and Bicknell WH, "Microcomputer control of Switched Reluctance Motor", IEEE Transactions on Industry Application, Vol. IA-22, No.4, July/August, 1986, pp 708-715.

4. D.E. Cameron, J.H. Lang & S. D. Umans, "The Origin of Acoustic Noise in Variable-Reluctance Motors", Industry Application Society meeting 1989, Vol.1, pp 108-115.

5. Chi-Yao Wu and Charles Pollock, "Analysis and Reduction of Vibrations and Acoustic Noise in the Switched Reluctance Drive", IEEE Tr. on Industry Application, Vol.31, No. 1, Jan/Feb 1995, pp 91-98.

6. D. E. Cameron, J. H. Lang and S. D. Umans, "The origin and Reduction of Acoustic Noise in Doubly Salient variable Reluctance Motors", IEEE

Tr. on Industry Application, Vol. 28, No.6, Nov/Dec 1992, pp 1250-1255.

7. C. Pollock and C. Y. Wu, "Acoustic Noise Cancellation Techniques for Switched Reluctance Drives", Industry Application Society meeting 1995, Vol.1, pp 448-455.

8. Mahn J., Williams D., Wong P., Horst G., Lioyd J., and Randall S., "Systematic Approach Toward Studying Noise and Vibration in Switched Reluctance Machines", IEEE, IAS Conf., San Diego, 1996, Vol 2, pp779-785.

9. Debiprasad Panda, V.Ramanarayanan, "An Accurate Position Estimation Method for Switched Reluctance Motor", IEEE conference on Power Electronics Drives and Energy System conference(PEDES-98), Australia.

10. Debiprasad Panda and V. Ramanrayanan, "Fuzzy logic based Control of Switched Reluctance Motor", International Conference on Signal

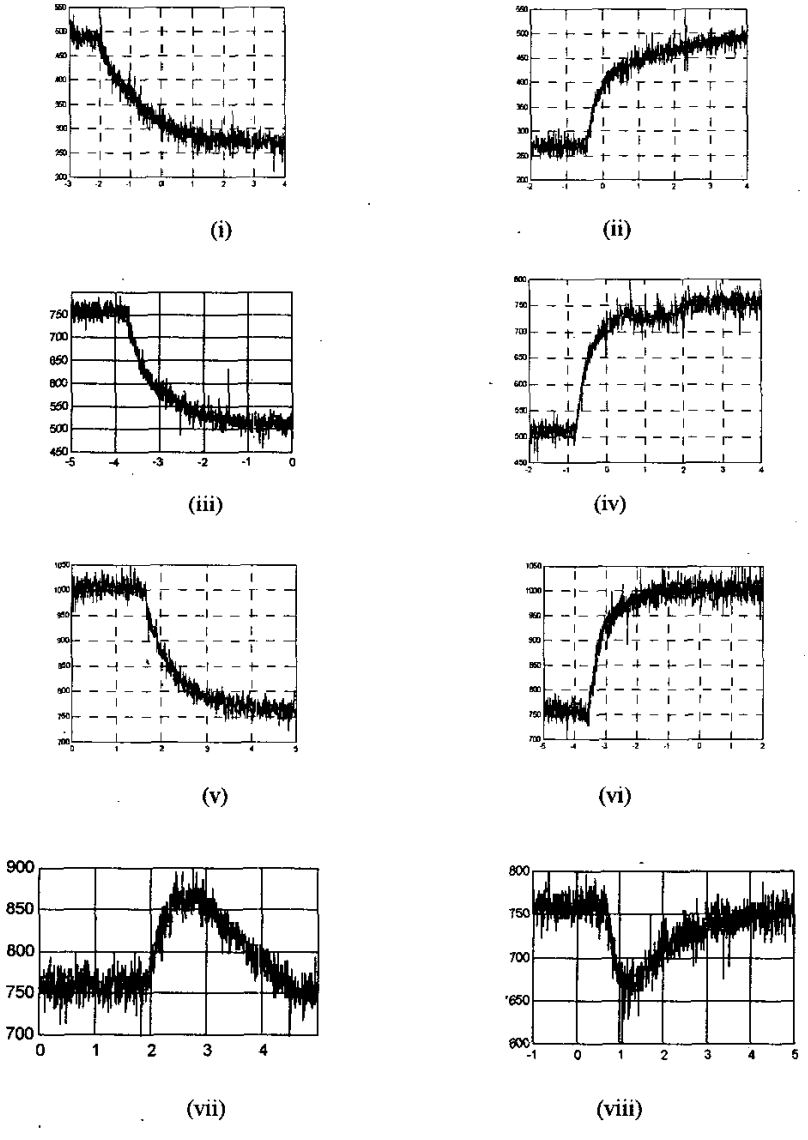

Fig. 8 Speed Transients: (i) 500 rpm to 250 rpm, (ii) 250 rpm to 500 rpm, (iii) 750 rpm to 500 rpm, (iv) 500 rpm to 750 rpm, (v) 1000 rpm to 750 rpm, (vi) 750 rpm to 1000 rpm, (vii) Speed Transient on Withdrawal of Load (10 Nm to 1 Nm), (viii) Speed Transient on Application of Load (1 Nm to 10 Nm). Horizontal Axes Represent Time in Seconds; Vertical Axes Represent Speed in rpm.